Available online at www.sciencedirect.com
SCIENCE DIRECT
ELSEVIER
Composites: Part B 37 (2006) 117–126
composites Part B: engineering
www.elsevier.com/locate/compositesb

Parameter identification of elastic interphase properties in fiber composites

A. Matzenmiller *, S. Gerlach

Institute of Mechanics, University of Kassel, D-34109 Kassel, Germany

Received 10 May 2004; revised 8 August 2005; accepted 18 August 2005

Abstract

The interphase region significantly influences the overall material behaviour of fiber composites as experimental investigations show. Since the interphase performance depends on the manufacturing process, their properties cannot be determined directly from bulk material specimen. Therefore, the elastic properties of the interphase are identified on the basis of a micromechanical model from the experimental data of the effective elasticity parameters of the homogeneous substitute material. By means of the generalised method of cells the average properties of the homogenised materials are related to the material parameters, the volume fractions and the geometrical arrangement of the individual phases. A third constituent besides the ones for fibers and matrix accounts for the interphase in the representative volume element. The model response is fitted best to the data with a gradient-based optimisation strategy, requiring the sensitivity analysis of the micromechanical model.

Keywords: B. Interface/interphase; C. Micro-mechanics; C. Numerical analysis; Identification of properties

1. Introduction

Numerous experimental studies in composite materials research focus on the investigation of the interphase with respect to its influence on the mechanical performance of the behaviour of composite materials, e.g. [1–4]. The tests show that the interphase has its own material properties, different from those of the matrix or the fibers, due to coatings on the fibers or chemical treatment of the fiber surface. As a consequence of the manufacturing process the interphase characteristics are in situ properties and cannot be measured directly in an experiment with specimen of the interphase material.

The search for the missing interphase parameters motivates the development of an identification strategy, based on a micromechanical approach with the interphase region as a third material component. In this paper the generalised method of cells (GMC) is used as the micromechanical model to quantify the overall effective properties of the composite with an elastic interphase region of finite thickness. Based on the analytical homogenisation scheme of the cells method, an identification algorithm is developed in Ref. [5], where the in situ properties of the interphase are determined from the effective properties of the composite and the parameters for the bulk material of the individual phases.

The inverse determination of the interphase properties from the effective material moduli requires the detailed knowledge of the microscopic structure of the composite. The elastic material parameters of the fibers and the matrix as well as the fiber volume fraction and the fiber architecture must be known or assumed. Additionally, the thickness of the interphase region has to be given or estimated. For a satisfying analysis the effective moduli of the composite should be measured, in order to account for the different manufacturing influences such as fiber surface treatment or for additional adhesives. With the results of the inverse identification for the interphase properties it is possible to evaluate the mechanical effect of the various manufacturing influences on the interphase characteristics.

2. Micromechanical model for elastic composites

The micromechanical modeling of inhomogeneous media aims at the determination of the effective (average) material properties for the equivalent homogeneous comparison material by means of the mechanical properties of the components and their geometrical arrangement in the composite. The description of the linear material behaviour is

* Corresponding author. Tel.: + 49 561 8042044; fax: +49 561 8042720.
E-mail address: amat@ifm.maschinenbau.uni-kassel.de (A. Matzenmiller).

1359-8368/$ - see front matter © 2005 Elsevier Ltd. All rights reserved.
doi:10.1016/j.compositesb.2005.08.003

based on the representative volume element (RVE), whose structure should be typical for the composite, small in comparison to the macrostructure and large with respect to the microstructure. The effective material properties are defined between the volume averaged stresses $\langle\boldsymbol{\sigma}\rangle$ and the averaged strains $\langle\boldsymbol{\varepsilon}\rangle$ of the composite with the elastic material stiffness tensor $\mathbb{C}^*$ and the compliance $\mathbb{S}^*$ of fourth order.

$$\langle\boldsymbol{\sigma}\rangle = \mathbb{C}^* : \langle\boldsymbol{\varepsilon}\rangle \quad \text{and} \langle\boldsymbol{\varepsilon}\rangle = \mathbb{S}^* : \langle\boldsymbol{\sigma}\rangle, \tag{1}$$

where the colon: stands for a double contraction and the parenthesis $\langle\ \rangle$ for the volume average according to

$$\langle\boldsymbol{\sigma}\rangle = \frac{1}{V}\int_V \boldsymbol{\sigma}(x)\mathrm{d}V \qquad \text{and} \langle\boldsymbol{\varepsilon}\rangle = \frac{1}{V}\int_V \boldsymbol{\varepsilon}(x)\mathrm{d}V \tag{2}$$

with x as the position vector of an arbitrary point in the material body. Since the averaged stress and strain components may only be computed from the exact solution of the stress and strain fields—see Eq. (2), simplifying assumptions must be made for the micromechanical models in order to find an approximation for the constitutive parameters of the composite. The usual micromechanical approach introduces the fourth order concentration tensors according to Hill. With the help of the phase-averaged strain concentration tensor $\mathbb{A}^{(i)}$ of fourth order a mathematical relationship is set up between the average strain tensor $\langle\boldsymbol{\varepsilon}^{(i)}\rangle$ in the individual phases (i) and the averaged strains $\langle\boldsymbol{\varepsilon}\rangle$ of the composite.

$$\langle\boldsymbol{\varepsilon}^{(i)}\rangle = \mathbb{A}^{(i)} : \langle\boldsymbol{\varepsilon}\rangle \tag{3}$$

with the definitions above the average stress of the elastic composite may be given in terms of the average composite strains. Hence, the effective stiffness of the $\mathbb{C}^*$ can be read off from Eq. (4)

$$\langle\boldsymbol{\sigma}\rangle = \sum_{i=1}^{N} c_i\mathbb{C}^{(i)} : \mathbb{A}^{(i)} : \langle\boldsymbol{\varepsilon}\rangle \tag{4}$$

in terms of the concentration tensors $\mathbb{A}^{(i)}$ and the stiffness tensors $\mathbb{C}^{(i)}$ of the material components:

$$\mathbb{C}^* = \sum_{i=1}^{N} c_i\mathbb{C}^{(i)} : \mathbb{A}^{(i)}, \tag{5}$$

where the scalars c_i represent the volume fractions and the integer N the number of phases.

The GMC, proposed by Paley and Aboudi [6], is used to calculate the concentration tensors—see Herakovich [7]. The cells model has proven to be very efficient in representing the elastic and inelastic behaviour of unidirectional fiber-reinforced composite materials—see Aboudi [8] or the recent example of application, given by the authors in Ref. [9]. A two-dimensional formulation suffices as a model for the composite with continuous fibers in the x_1-direction. The fibers are arranged double periodically in the x_2–x_3-plane—see Fig. 1(a)—leading to orthotropic material symmetry. The necessary corrections of the associated material properties are given at the end of this section by means of Eq. (17).

Due to the assumption above it is possible to identify a unit cell as a RVE for the square arrangement of fibers with strong periodicity. In the following the term RVE is not only restricted to a representative zone of the composite with randomly distributed fibers, but is also used as a synonym for the unit cell of periodically arranged fibers. The unit cell is divided into an arbitrary number of sub-domains, called subcells (Fig. 1b) with dimensions h_β and l_γ. In the framework of the two-dimensional formulation it is assumed that the average subcell strains in fiber direction $\langle\varepsilon_{11}^{(\beta\gamma)}\rangle$ are equal to the average composite strain in fiber direction $\langle\varepsilon_{11}\rangle$. This assumption corresponds to the conception of the simple Voigt model, i.e. the GMC results for the axial elasticity modulus E_a^* and the axial Poisson ratio ν_a^* conform to this simple rules of mixture. The two-dimensional formulation of the method of cells represents a generalised plane strain model (ε_{11} = constant, $\varepsilon_{31} = \varepsilon_{32} = 0$), because the resulting out-of-plane displacements varies linearly with

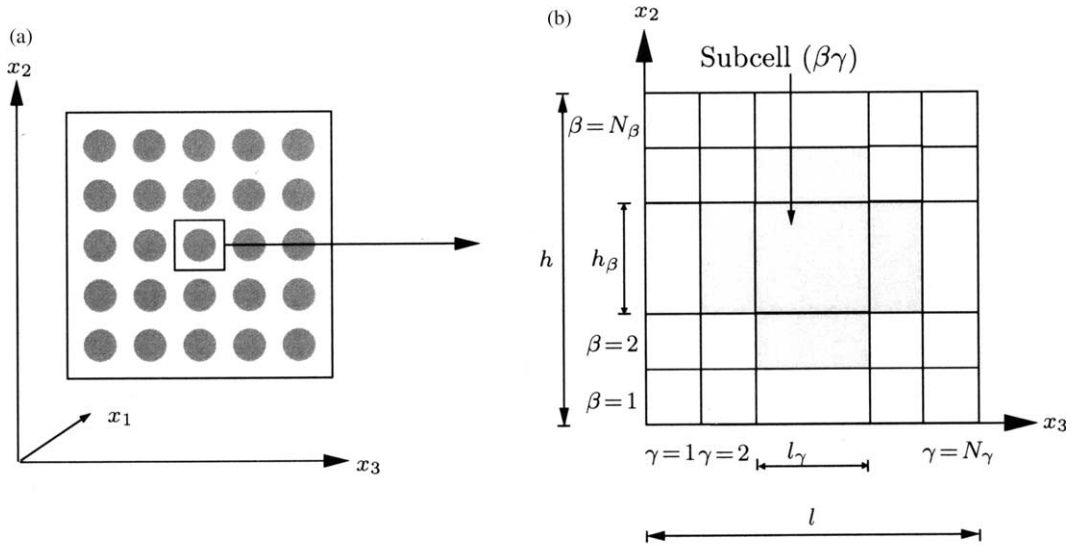

Fig. 1. (a) Composite with double periodic array of fibers in x_1-direction, (b) Representative volume element with subcells and nomenclature.

respect to the position of the x_2–x_3-plane. If the results of the GMC model are compared with the homogenised properties computed by the finite element method, generalised plane strain conditions should be used for the modeling of the unit cell. Therewith the theoretical assumptions of the GMC and the FE-model match best possible and the results of the two homogenisation techniques are comparable. The generalised plane strain conditions take into account, that the x_2–x_3-planes remain plain and perpendicular to the fibres axes but can move axially. In the case of pure transverse loading for example, the axial force resulting from the axial micro-stresses vanishes. By applying plane strain conditions ($\varepsilon_{11}=\varepsilon_{31}=\varepsilon_{32}=0$) an axial force appear due to a transverse loading. Therefore the behaviour of the finite element model would be stiffer and the calculated properties of the composite would be smaller than the results for the model with generalised plane strain conditions.

The implementation of a generalised plane strain model for the considered unit-cell with finite elements can be achieved by making use of special elements like the PLANE182-Element in ANSYS or alternatively by modeling one row of three-dimensional brick elements with coupled displacements in the out-of-plane direction. The latter possibility were used in this work.

Within each subcell, subscripted with the index pair ($\beta\gamma$), a bilinear displacement field is assumed and formulated in the local coordinate systems. The material behaviour of the cells shall be either isotropic or transversely isotropic. Continuity of the displacements u_i is required at the interfaces between the subcells of the RVEs as well as at the boundaries between adjacent RVEs. The continuity conditions can be written compactly in matrix form in terms of the phase averaged strains $\langle\varepsilon_s\rangle$ and the effective strains $\langle\varepsilon\rangle$ of the composite—see Herakovich [7] or Paley and Aboudi [6] for further details.

$$\mathbf{A}_G\langle\boldsymbol{\varepsilon}_s\rangle = \mathbf{J}\langle\boldsymbol{\varepsilon}\rangle. \tag{6}$$

The coefficients of the matrices A_G and J result from the geometry of the subcells in the RVE. $\langle\boldsymbol{\varepsilon}_s\rangle$ is the column vector of the averaged unknown strain components $\langle\boldsymbol{\varepsilon}^{(\beta\gamma)}\rangle$ in all $N_\beta N_\gamma$-subcells:

$$\langle\boldsymbol{\varepsilon}_s\rangle^T := (\langle\boldsymbol{\varepsilon}^{(11)}\rangle, \langle\boldsymbol{\varepsilon}^{(12)}\rangle, \ldots, \langle\boldsymbol{\varepsilon}^{(N_\beta N_\gamma)}\rangle)^{\mathbf{T}} \tag{7}$$

The averaged strain tensor $\langle\boldsymbol{\varepsilon}^{(\beta\gamma)}\rangle$ in subcell ($\beta\gamma$) equals the volume averaged strain components $\langle\varepsilon_{ij}^{(i)}\rangle$ in phase (i), which fills up the whole cell.

$$\langle\boldsymbol{\varepsilon}^{(\beta\gamma)}\rangle^{\mathbf{T}} := (\langle\varepsilon_{11}\rangle, \langle\varepsilon_{22}\rangle, \langle\varepsilon_{33}\rangle, \langle\varepsilon_{23}\rangle, \langle\varepsilon_{13}\rangle, \langle\varepsilon_{12}\rangle)^{\mathbf{T}} \tag{8}$$

The tensor $\langle\boldsymbol{\varepsilon}\rangle$ represents the averaged strain components in vector notation of the homogenised comparison material according to Eq. (2). The equilibrium conditions read for the phase averaged stresses $\langle\boldsymbol{\sigma}^{(\beta\gamma)}\rangle$ at the interfaces of the subcells in the RVE:

$$\langle\sigma_{j2}^{(\beta\gamma)}\rangle = \langle\sigma_{j2}^{(\hat{\beta}\gamma)}\rangle \tag{9}$$

$$\langle\sigma_{j3}^{(\beta\gamma)}\rangle = \langle\sigma_{j3}^{(\beta\hat{\gamma})}\rangle \tag{10}$$

with $j=1, 2, 3$; $\beta=1,\ldots,N_\beta$ and $\gamma=1,\ldots,N_\gamma$. N_β and N_γ denote the number of subcells in each direction and $\hat{\beta}$ and $\hat{\gamma}$ are defined as:

$$\hat{\beta} = \begin{cases} \beta+1, & \beta < N_\beta \\ 1, & \beta = N_\beta \end{cases} \quad \text{and} \quad \hat{\gamma} = \begin{cases} \gamma+1, & \gamma < N_\gamma \\ 1, & \gamma = N_\gamma \end{cases}. \tag{11}$$

Eqs. (9) and (10) can be written in matrix form with the help of Eqs. (7) and (8) according to references [7] or [6]:

$$\mathbf{A}_M\langle\boldsymbol{\varepsilon}_s\rangle = 0. \tag{12}$$

The matrix A_M contains only known coefficients, depending on the material parameters of the constituents. Eqs. (6) and (12) may be combined in the following relationship in vector notation between the individual strains in all subcells $\langle\boldsymbol{\varepsilon}_s\rangle$ and the macroscopic strains is in the homogenised composite $\langle\boldsymbol{\varepsilon}\rangle$:

$$\langle\boldsymbol{\varepsilon}_s\rangle = \mathbf{A}\langle\boldsymbol{\varepsilon}\rangle \quad \text{with the definition :}$$
$$\mathbf{A} = \begin{bmatrix} \mathbf{A}_G \\ \mathbf{A} \end{bmatrix}^{-1} \begin{bmatrix} \mathbf{J} \\ 0 \end{bmatrix} = \hat{\mathbf{A}}^{-1}\mathbf{K}, \tag{13}$$

where $\hat{\mathbf{A}}$ is an auxiliary matrix, written as

$$\hat{\mathbf{A}} = \begin{bmatrix} \mathbf{A}_G \\ \mathbf{A}_M \end{bmatrix} \tag{14}$$

and K is part of the right hand side of Eqs. (6) and (12).

$$\mathbf{K} = \begin{bmatrix} \mathbf{J} \\ 0 \end{bmatrix} \tag{15}$$

The matrix $\mathbf{A}$ comprises the elements of the fourth order concentration tensors $\mathbb{A}^{(\beta\gamma)}$ for all subcells written in matrix form $\mathbf{A}^{(\beta\gamma)}$. The matrix $\mathbf{C}^*$ for the effective stiffness tensor $\mathbb{C}^*$ of the composite is finally calculated from the matrices $\mathbf{A}^{(\beta\gamma)}$ and $\mathbf{C}^{(\beta\gamma)}$, the concentration and stiffness tensors of the cells.

$$\mathbf{C}^* = \frac{1}{hl}\sum_{\beta=1}^{\beta=N_\beta}\sum_{\gamma=1}^{\gamma=N_\gamma} h_\beta l_\gamma \mathbf{C}^{(\beta\gamma)}\mathbf{A}^{(\beta\gamma)} \tag{16}$$

For the square arrangement of the fibers Eq. (16) provides the characteristics of an orthotropic composite material with three axes of symmetry. Unidirectionally reinforced fiber composites are usually assumed to exhibit transversely isotropic symmetry characteristics in the macroscopic sense. Aboudi [10] evaluates the transversely isotropic properties by averaging the stiffness tensor of the orthotropic symmetry over the rotation angle ξ. According to Aboudi the components of the stiffness tensor C^{TI} for the transversely isotropic material can be calculated as follows from the components of the stiffness tensor C^{Ort} for orthotropic material behaviour in

Voigt notation:

$$
\begin{aligned}
&C_{11}^{\mathrm{TI}} = C_{11}^{\mathrm{Ort}} \qquad C_{12}^{\mathrm{TI}} = C_{12}^{\mathrm{Ort}} \\
&C_{22}^{\mathrm{TI}} = 0.75C_{22}^{\mathrm{Ort}} + 0.25C_{23}^{\mathrm{Ort}} + 0.5C_{66}^{\mathrm{Ort}} \\
&C_{23}^{\mathrm{TI}} = 0.25C_{22}^{\mathrm{Ort}} + 0.75C_{23}^{\mathrm{Ort}} - 0.5C_{66}^{\mathrm{Ort}} \qquad C_{44}^{\mathrm{TI}} = C_{44}^{\mathrm{Ort}} \\
&C_{66}^{\mathrm{TI}} = 0.5(C_{22}^{\mathrm{TI}} - C_{23}^{\mathrm{TI}})
\end{aligned}
\tag{17}
$$

The transformations in Eq. (17) enforce the material properties for linear elastic transverse isotropy. Alternatively, a hexagonal arrangement of the microstructure can be used to achieve transverse isotropy of the homogeneous composite. The physically linearised constitutive equations are the same for elastic materials with hexagonal or transverse isotropic material symmetries. Hence, the macroscopically transverse isotropic material behaviour may be determined form the hexagonal arrangement of the fibers. In Fig. 2 the square and the hexagonal arrangement of the fibers are shown. By making use of the periodicity property of the unit cell, two different possibilities are given for the associated RVE for the hexagonal fiber arrangement. The rectangular unit cell for the hexagonal architecture may be simply modelled with subcells by the GMC method. The choice for the RVE in the case of the double periodical square assemblage is obvious and also depicted in Fig. 2a. The four subcells of the RVE in the square arrangement are also shown in Fig. 2a. The results of the GMC method for elastic fiber and matrix behaviour with perfect bonding is given for the hexagonal arrangement with the rectangular unit cell and for the square arrangement with successive transformation to transverse isotropy for the effective transverse elasticity modulus E_t^* in Fig. 2b. The results of both methods do not differ significantly.

The identification of the interphase properties by means of the sensitivity analysis for the parameters is much more elaborate for the hexagonal unit cell as for the RVE of the square arrangement. Hence, the simpler unit cell is used for the identification task.

3. Interphase model with finite thickness

The GMC allows the modeling of arbitrary shaped inclusions in a matrix. Therefore, the interphase region, comprising the material adjacent to the bond, may by taken into account as a thin layer of subcells between the fiber and the matrix phase. For instance the GMC model with the interphase for the example below consists of 13 by 13 subcells in total as shown in Fig. 3. This unit cell represents the square arrangement of approximately circular fibers in the composite and the transversely isotropic properties of the macroscopic behaviour are achieved by the transformation rule (17). In view of the identification procedure with gradient based solution algorithms the unit cell for cell for the three phases is kept as simple as possible to solve the related inverse problem. Even the RVE for the hexagonal arrangement of the fibers with a thin interphase is much more elaborate to analyse and may be investigated in future. Besides this additional effort the hexagonal model does still not satisfy the requirement of a RVE to be statistically typical for the microstructure, as the hexagonal arrangement of the fibers is based on strong periodicity. Therefore, a much bigger region of the composite should be considered including more heterogeneities and varying fiber arrangements must be investigated. In this analysis a simple unit cell is chosen for the purpose of demonstrating the inverse identification strategy developed.

The isotropic constitutive behaviour of the constituents is described by the bulk shear moduli K and G of the three phases. In order to account for the deviating interphase properties, a scalar κ is introduced to relate the isotropic interphase

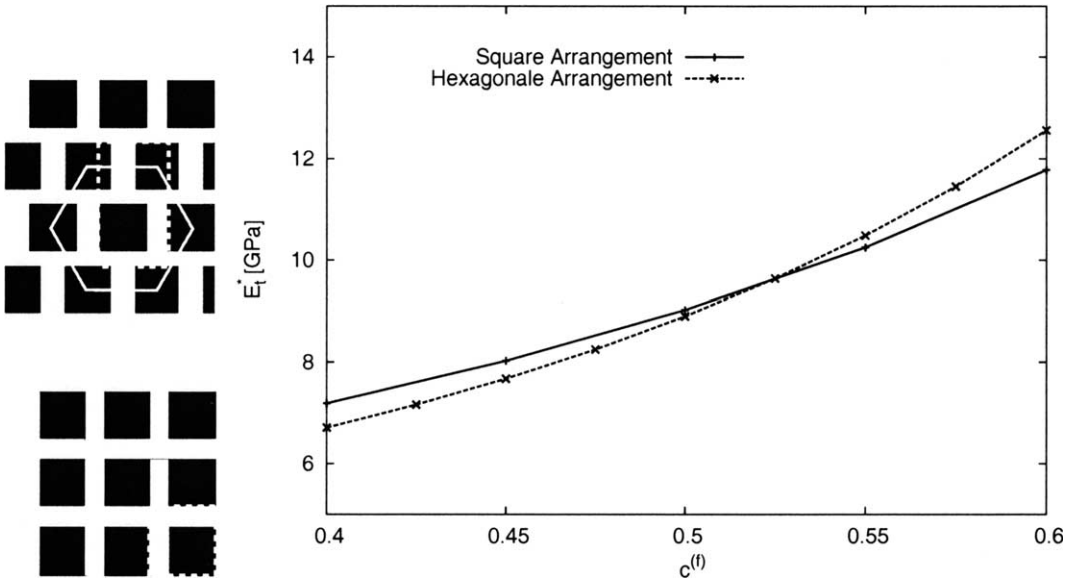

Fig. 2. (a) Square and hexagonal arrangement of a square fiber (b) Comparision of the effective transverse elasticoity modulus E_t^* for the two different arrangement with GMC.

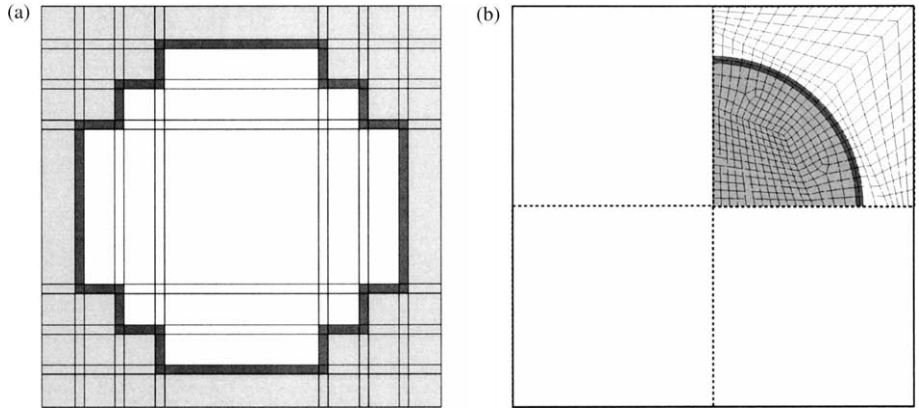

Fig. 3. RVE with interphase modeled by (a) GMC and (b) FEM.

properties $K^{(i)}$, $G^{(i)}$ to the isotropic elasticity parameters $K^{(m)}$, $G^{(m)}$ of the matrix:

$$K^{(i)} = \kappa K^{(m)} \tag{18}$$

$$G^{(i)} = \kappa G^{(m)} \tag{19}$$

This simplification is based on the assumption that the Poisson numbers for the matrix and the interphase material are equal. Due to the absence of shear coupling between the subcells in the GMC model this approach cannot be applied meaningfully when the interphase properties are substantially lower than the fiber and matrix phases.

4. Identification algorithm

The stiffness properties of the interphase region are found by optimising an objective function f_{LS}, typically set up in identification theory with the help of the least-square method as the error between the data, denoted as d_i in the general case, and the model response M_i, which depends on the unknown parameterκ.

$$f_{LS}(\kappa) = \frac{1}{2}\sum_{i=1}^{N_d}(M_i(\kappa) - d_i)^2 \tag{20}$$

The vector components d_i comprise the experimental data, which can be only a single quantity or a number of values from the N_d different experimental measurements. $M_i(\kappa)$ represents the model function, evolving from the underlying micro-mechanical method and depending on the interphase scalar κ. According to Eqs. (16), (18) and (19) the model function depends on the effective stiffness tensor $\mathbf{C}^*$ of the composite in our case:

$$M_i(\kappa) = f_i(\mathbf{C}^*(\kappa)) \tag{21}$$

with the overall composite stiffness as a function of the elastic interphase parameter κ.

$$\mathbf{C}^*(\kappa) = \frac{1}{hl}\sum_{\beta=1}^{\beta=N_\beta}\sum_{\gamma=1}^{\gamma=N_\gamma} h_\beta l_\gamma \mathbf{C}^{(\beta\gamma)}(\kappa)\mathbf{A}^{(\beta\gamma)}(\kappa). \tag{22}$$

Obviously, $M_i(\kappa)$ is a function of the interphase parameter κ through the components of the effective stiffness tensor $\mathbb{C}^*$. The effective transverse material stiffness E_t^* is chosen as the key quantity for the identification of the interphase properties of the model in this study. The E_t^*-modulus of the composite can be expressed by means of the interconversion rules in terms of the components for the linear elastic, transverse isotropic stiffness tensor $\mathbb{C}^*$, derived from the phase properties by means of the micromechanical model.

$$M_1(\kappa) = E_t^*(\kappa) = \{C_{11}^*(\kappa)[C_{22}^*(\kappa) + C_{23}^*(\kappa)] - (C_{23}^*(\kappa))^2\}\frac{C_{22}^*(\kappa) - C_{23}^*(\kappa)}{C_{11}^*(\kappa)C_{22}^*(\kappa) - (C_{12}^*(\kappa))^2} \tag{23}$$

Note, the parameter κ is determined inversely by fitting the model response best to the experimental data, i.e. minimising the least-square functional f_{LS} in Eq. (20). Therefore, also possible modeling errors or experimental uncertainties, like measurement errors or geometrical imperfections, are assigned to this parameter κ.

5. Optimisation algorithm

The unknown parameter κ is evaluated by solving a nonlinear optimisation task with the object function in (20) and the non-negative constraint: $\kappa \geq 0.0$. The sequential quadratic programming (SQP) of Ref. [11] is used here to minimise the objective function. The SQP-method is based is based on the idea that the given nonlinear optimisation task is replaced by a sequence of quadratic subproblems, which can be solved more easily. This solution procedure can be applied, if the number of unknowns at hand is not too large, the function value and the gradient can be computed sufficiently accurately, and if the model response is 'smooth' and well-conditioned. The necessary gradient of the function is determined analytically, i.e. a sensitivity analysis supplies the derivatives of the objective function with respect to the unknown parameter κ.

5.1. Sensitivity analysis of the micromechanical model

The gradient of the objective function (20) with respect to the unknown parameter κ is given by derivative:

$$g(\kappa) := \frac{\mathrm{d}f_{\mathrm{LS}}(\kappa)}{\mathrm{d}\kappa} = \sum_{i=1}^{N_d} (M_i(\kappa) - d_i) \frac{\mathrm{d}M_i(\kappa)}{\mathrm{d}\kappa} \tag{24}$$

The derivative of the model Eq. (21) yields:

$$\frac{\mathrm{d}M_i(\kappa)}{\mathrm{d}\kappa} = \frac{\mathrm{d}f_i(\mathbf{C}^*(\kappa))}{\mathrm{d}\kappa} \tag{25}$$

According to the product rule of differential calculus the parameter derivative of the effective stiffness matrix is composed of two parts:

$$\frac{\mathrm{d}\mathbf{C}^*(\kappa)}{\mathrm{d}\kappa} = \frac{1}{hl} \sum_{\beta=1}^{\beta=N_\beta} \sum_{\gamma=1}^{\gamma=N_\gamma} h_\beta l_\gamma \left[\frac{\mathrm{d}\mathbf{C}^{(\beta\gamma)}(\kappa)}{\mathrm{d}\kappa} \mathbf{A}^{(\beta\gamma)}(\kappa) + \mathbf{C}^{(\beta\gamma)}(k) \frac{\mathrm{d}\mathbf{A}^{(\beta\gamma)}(\kappa)}{\mathrm{d}\kappa} \right] \tag{26}$$

The first part represents the sensitivities of the stiffness matrices of the subcells with respect to the parameter κ. For the subcells of the interphase region it follows from Eqs. (18) and (19):

$$\frac{\mathrm{d}\mathbf{C}^{(\beta\gamma)}(\kappa)}{\mathrm{d}\kappa} = \mathbf{C}^{(m)}, \quad \text{if } \mathbf{C}^{(\beta\gamma)} = \mathbf{C}^{(i)} = \kappa \cdot \mathbf{C}^{(m)}. \tag{27}$$

For the fiber or matrix subcells the derivative in Eq. (27) vanishes. The second part of the sum in Eq. (26) corresponds to the parameter derivative of the concentration tensors $\mathbb{A}^{(\beta\gamma)}$ of the cell with in indices $\beta\gamma$. These tensors are stored as submatrices $\mathrm{A}^{(\beta\gamma)}$ in the matrix A, defined in Eq. (13). The defining equation of A leads to:

$$\frac{\mathrm{d}\mathbf{A}}{\mathrm{d}\kappa} = \begin{bmatrix} \mathbf{A}_G \\ \mathbf{A}_M \end{bmatrix}^{-1} \frac{\mathrm{d}}{\mathrm{d}\kappa} \begin{bmatrix} \mathbf{J} \\ \mathbf{0} \end{bmatrix} + \frac{\mathrm{d}}{\mathrm{d}\kappa} = \begin{bmatrix} \mathbf{A}_G \\ \mathbf{A}_M \end{bmatrix}^{-1} \begin{bmatrix} \mathbf{J} \\ \mathbf{0} \end{bmatrix}$$

$$= \frac{\mathbf{d}}{\mathbf{d}\kappa} (\hat{\mathbf{A}}^{-1}\mathbf{K}) = \hat{\mathbf{A}}^{-1} \frac{\mathrm{d}\mathbf{K}}{\mathrm{d}\kappa} + \frac{\mathrm{d}\hat{\mathbf{A}}^{-1}}{\mathrm{d}\boldsymbol{\kappa}} \mathbf{K} \tag{28}$$

The first term in the sum above disappears, since the submatrix J is independent of the parameter κ. The parameter derivative of the inverse matrix $\hat{\mathbf{A}}^{-1}$ in the second term can be derived from the identity $\hat{\mathbf{A}}\hat{\mathbf{A}}^{-1} = \mathbf{I}$:

$$\frac{\mathrm{d}\hat{\mathbf{A}}^{-1}}{\mathrm{d}\kappa} = -\hat{\mathbf{A}}^{-1} \frac{\mathrm{d}\hat{\mathbf{A}}}{\mathrm{d}\kappa} = \hat{\mathbf{A}}^{-1}. \tag{29}$$

The inverse $\hat{\mathbf{A}}^{-1}$ follows from by Eq. (14), which also furnishes the parameter derivative of the auxiliary matrix $\hat{\mathbf{A}}$:

$$\frac{\mathrm{d}\hat{\mathbf{A}}}{\mathrm{d}\kappa} = \frac{\mathrm{d}}{\mathrm{d}\kappa} \begin{bmatrix} \mathbf{A}_{\mathrm{G}} \\ \mathbf{A}_{\mathrm{M}} \end{bmatrix} = \begin{bmatrix} \mathbf{0} \\ \dfrac{\mathrm{d}\mathbf{A}_{\mathrm{M}}}{\mathrm{d}\kappa} \end{bmatrix}. \tag{30}$$

Since the submatrix $\mathrm{A_G}$ comprises the geometrical quantities of the RVE, only the components of the submatrix $\mathrm{A_M}$ provide in general non-zero contributions to the derivative. The computation for the various examples below showed practice that the numerical values of the derivative of the concentration matrices in Eq. (26) are close to zero and may be neglected in comparison to the first part of the sum, further outlined in Eq. (27). This simplification substantially reduces the computational effort.

6. Numerical examples

Two examples are given to prove the success of the identification approach and secondly to solve a real problem. For demonstration purposes the data d_i for the identification step are computed from the model response $M_i(\kappa)$ for a fixed value of the interphase parameter $\bar{\kappa}$ with the finite element method (FEM). Afterwards the parameter κ is identified from the data d_i and the model response $M_i(\bar{\kappa})$ and finally compared to the chosen value $\bar{\kappa}$.

6.1. Test example with simulated data from FEM model

In the first example the effective transverse elasticity modulus E_t^*, taken for the input data d_i of the identification task, is calculated for a number of preselected values $\kappa = \bar{\kappa}$. A square shaped unit cell is chosen with a single fiber, surrounded by a thin interphase region of thickness $t^{(i)}$ and embedded into the matrix material—see Fig. 3(b). By making use of the symmetry conditions and the periodic nature of the unit cell, the FE-model in Fig. 3(b) corresponds to a square distribution of the fibers as shown in Fig. 1(a). Therefore, the composite has cubic symmetry resulting in orthotropic material behaviour with 6 independent elastic constants.

The effective properties of the composite are calculated from the solution of the boundary value problem for the RVE, analysed with the finite element program ANSYS. The effective transverse elasticity modulus E_t^* of the composite model is determined for a fixed parameter $\bar{\kappa}$ on the basis of Hill's macro-homogeneity condition, which assumes that the strain energy of the original heterogeneous material is equivalent to the one of the homogenised substitute material. For further details the interested reader can be referred to [12] and [13].

The overall transverse elasticity modulus E_t^* of the composite model is calculated for four different values of the fiber volume content $c^{(\mathrm{f})}$ between 0.3 and 0.6 and five different values of the interphase property $\bar{\kappa}$ by means of the finite element model in Fig. 3(b). The modulus $E_t^*(\bar{\kappa})$ is used as the input datum d_i in the objective function (20) for the reidentification of the interphase parameter κ with the GMC model in Fig. 3(a) of the demonstration example.

$$d_i \equiv E_t^*(\bar{\kappa}) \tag{31}$$

The elastic properties of the isotropic material phases are taken from Herakovich [7] (for the fibers: $E^{(\mathrm{f})} = 113.4$ GPa, $\nu^{(\mathrm{f})} = 0.22$, and for the matrix: $E^{(\mathrm{m})} = 5.35$ GPa, $\nu^{(\mathrm{m})} = 0.35$). The fiber radius is chosen as $\mathrm{r}^{(\mathrm{f})} = 6$ μm and the interphase

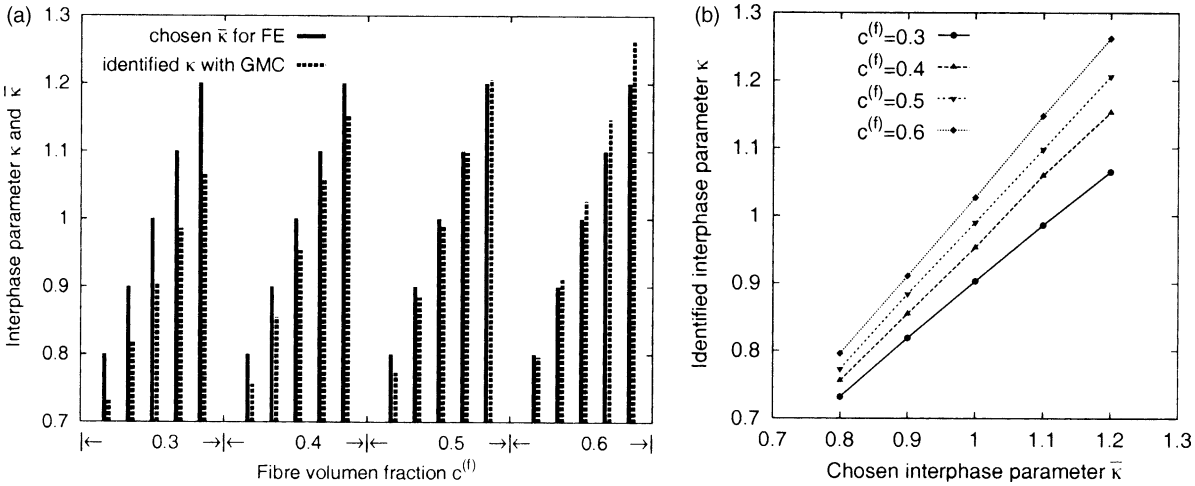

Fig. 4. Results of identifed parameter κ and comparison to the chosen $\bar{k}$.

thickness is assumed to $t^{(i)}=0.3$ μm. The influence of the interphase properties are studied by taking five different values $\bar{\kappa}$ for the interphase parameter between 0.8 and 1.2 in steps of 0.1. A total of twenty runs is performed.

The diagram in Fig. 4(a) shows the reidentified interphase parameter κ in comparison to the given interphase parameter $\bar{\kappa}$ for the FE-calculation of E_t^*.

The fairly good agreement between the chosen values for $\bar{\kappa}$ and the identified results κ confirms that GMC model is capable to determine results close to the FE-modell with less computational effort, as shown already by Aboudi [14] or Arnold et al. [15]. The identified interphase parameter κ is plotted versus the corresponding chosen value $\bar{\kappa}$ in Fig. 4(b). Ideally, the graph should coincide with the first diagonal. However, the plotted graphs are below the diagonal and, thus, indicate that the identified values are always a little smaller than the chosen ones, which could be caused by the absence of shear coupling in the GMC model and the tendency for stiffer results of the finite elements, if they are based on the irreducible displacement method. Nevertheless, the successful application of the proposed identification algorithm is proven.

6.2. Identification of interphase properties from experimental data

In the second example the interphase properties are identified with the experimental data E_t^* of Wacker in Refs. [2,16] for the transverse elasticity modulus. In addition Wacker specifies experimentally the elastic material parameters of the fibers and the matrix and gives the fiber volume content $c^{(f)}$, the fiber radius $r^{(f)}$ as well as the range of the interphase thickness $t^{(i)}$. All values are summarised in Table 1.

Furthermore the effective transverse elasticity modulus E_t^* for the input d_i of the identification task was determined from tension tests transverse to the fiber direction for four different cases of fiber surface treatment, distinguished by the notation: A1128, PU, EP, PE. The measured modulus E_t^* is listed for each material system in column 3 of Table 2. The properties of the interphase region in the tested composites vary due to the different surface treatments and because of unavoidable material imperfections. The average stiffness of the interphase region can be evaluated with the micromechanical GMC-model by solving the inverse problem on the basis of the experimentally found properties of the individual phases, given in Table 1 together with the test data for the transverse elasticity modulus E_t^* of the composite and the fiber volume fraction $c^{(f)}$.

The identified results of the interphase parameter κ are listed in columns four to six of Table 2 for three different values of the interphase thickness $t^{(i)}$. In the first case the values for κ are identified from the model of transverse isotropy based on the transformation according to Eq. (17). The values in parenthesis for κ are identified from the orthotropic material model without the transformation according to Eq. (17).

The summary of the results in Table 2 shows that the objective function could be solved for a given interphase thickness of $t^{(i)}=0.3$ μm only in two cases and for $t^{(i)}=0.4$ μm in three cases, if transverse isotropy is assumed in the GMC-model.

For the case of the interphase thickness $t^{(i)}=0.7$ μm and the assumption of transverse isotropy a finite positive value for the parameter κ could be found for all combinations of given fiber volume fraction and surface treatment—see column six. However, if orthotropic material symmetry is assumed, the scalar κ may be identified for all given thickness values $t^{(i)}$ as shown by the results in parenthesis of columns four to six of Table 2.

In Fig. 5(a) and (b) the graphs of the transverse elastic moduli E_t^{Ort} and E_t^{TI}, calculated with the GMC-model of the composite in Fig. 3(a), are plotted as functions of the interphase

Table 1
Specific values for the material phases of the fiber-reinforced composite in Ref. [2]

Material phase	Specific properties		
Glass fiber (E-glass)	$E^{(f)}=77$ GPa,	$\nu^{(f)}=0.2$,	$r^{(f)}=6$ μm
Epoxy resin 556/917	$E^{(m)}=3.11$ GPa	$\nu^{(m)}=0.34$	
Interphase thickness	$t^{(i)}=0.3$–0.7 μm		

Table 2
Experimental values of E_t^* and identified interphase parameters κ with and without transformation of the effective material parameters

Material	Volume fraction $c^{(f)}$ [%]	E_t^* (MPa)	Interphase parameter (κ)		
			$T^{(i)}=0.3$ μm	$t^{(i)}=0.4$ μm	$t^{(i)}=0.7$ μm
556/917 A1128	52.0	11335	−(1.96)	−(1.43)	2.55 (1.20)
556/917 PU	39.3	7193	10.9 (0.78)	3.42 (0.823)	1.72 (0.87)
	43.6	8941	−(2.63)	−(1.94)	4.06 (1.36)
	53.1	12057	−(2.63)	−(1.82)	2.85 (1.33)
556/917 EP	50.7	10269	−(1.14)	5.96 (1.07)	1.92 (0.99)
556/917 PE	46.2	7449	0.76 (0.36)	0.80 (0.42)	0.85 (0.55)

parameter κ for the assumption of an orthotropic material symmetry $E_t^{\mathrm{Ort}} = \hat{E}_t^{\mathrm{Ort}}(\kappa)$ as well as for the transverse isotropic case $E_t^{\mathrm{TI}} = \hat{E}_t^{\mathrm{TI}}(\kappa)$. For the latter supposition the elastic modulus E_t^{TI} is computed from the components of the stiffness matrix for orthotropic symmetry in accordance with the transformation formula (17). The data sets for the fiber-matrix-interphase-systems 556/917PE and 556/917EP with the interphase thickness $t^{(i)}=0.3$ μm are used to demonstrate the success and the difficulties with the identification of the interphase parameter κ.

For the material system 556/917 PE with the test results $E_t^* = 7.449$ GPa of the transverse elastic modulus and fiber volume fraction $c^{(f)}=0.307$ the solution point for the associated interphase parameter κ is marked by a black square on the graph of the model response for the transverse isotropic case ($\kappa=0.76$) and by a triangle for the orthotropic one ($\kappa=0.36$) in Fig. 5(a). The symbols indicate the intersection of the horizontal line through the experimental result for E_t^* of Wacker [2] with the graphs of the functions $\hat{E}_t^{\mathrm{TI}}(\kappa)$ and $\hat{E}_t^{\mathrm{Ort}}(\kappa)$ from the parameter study of the GMC-model for the two symmetry assumptions.

In Fig. 5(b) an example of an non successful identification is presented by the material system 556/917 EP with fiber volume content $c^{(f)}=0.507$ and measured $E_t^* = 10.269$ GPa. The curve of the transverse isotropic modulus E_t^{TI} as a function of κ does not attain the experimentally measured value E_t^* for the case of the interphase thickness $t^{(i)}=0$, 3 μm even for very large and, thus, unrealistic values of κ. However, for orthotropic material symmetry the scalar κ is computed to $\kappa=1.14$ as indicated by the triangle in Fig. 5(b).

The example shows that the identification procedure works successfully, if the input data allow a solution. However, not all investigations are satisfying, since for some sets of input data for the fiber-matrix-interphase system the optimisation problem has no solution or the identified interphase parameter κ is unexpectedly large. Since the interphase thickness is small, minor errors of the material parameters for the matrix and the fibers, of the experimental data and the geometrical measures cause significant changes of the parameter κ.

The results in Refs. [2,16] for the interfacial stiffness could not be accomplished. First, the authors in [16] use standard linear triangular elements, which tend to be very stiff. Then the interphase parameter must be low to compensate for the stiff finite element mesh. Hence, the interphase stiffness parameter κ is underestimated.

Another reason for the successful identification in Ref. [2, 16] is due to the fact that the FE-model there is based on a RVE with a square arrangement of the fibers. Therefore, the computed elasticity modulus of Wacker represents the transverse elastic modulus of the composite with an orthotropic material symmetry. The elastic modulus E_t transverse to the fiber is calculated from the micromechanical model of Ref.

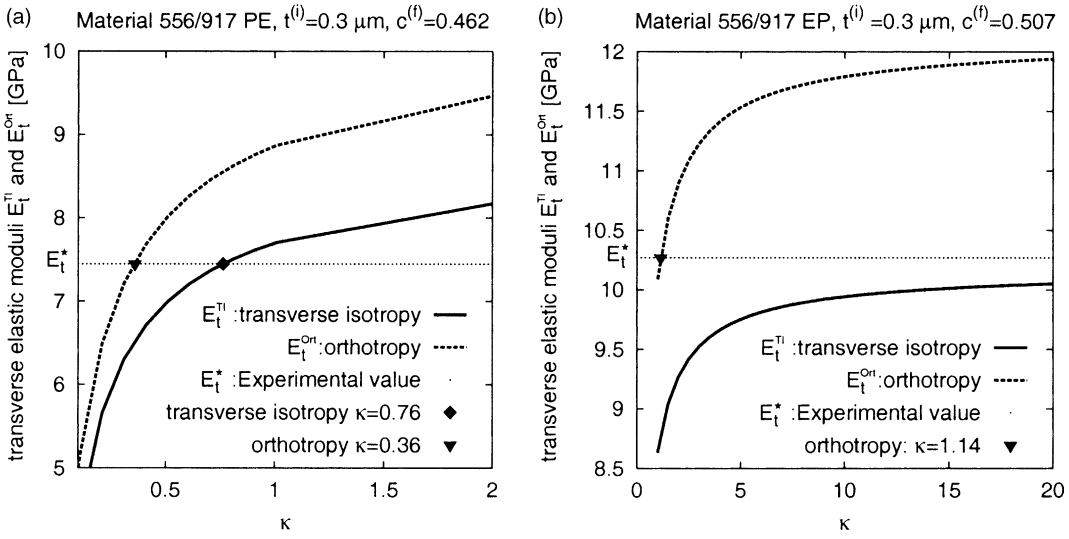

Fig. 5. Transverse elastic modulus for transverse isotropy $E_t^* = E_t^{TI}$ and or-thotropy $E_t^* = E_t^{Ort}$ as function of parameter κ and experimental result $E_t^\star$ of [2].

[10] for transverse isotropic material symmetry by applying the transformation rule in Eq. (17) to the stiffness components of the composite with orthotropic symmetry. The elastic modulus E_t^{TI} transverse to the fiber for the assumption of transversal isotropy is about 12–20% smaller than the corresponding elastic one E_t^{Ort} for orthotropy. Therefore, a larger value for the interphase stiffness κ is identified, which makes up the low estimate of the effective elastic modulus E^{TI} from the transverse isotropic model.

Even for the case of a rigid interphase the resulting transverse elasticity moduli E^{TI} and E^{Ort} remain finite. Thus, the functions $\hat{E}_t^{\mathrm{TI}}(\kappa)$ and $\hat{E}_t^{\mathrm{Ort}}(\kappa)$ are bounded from above. In the case of Fig. 5(b) the upper limit of E_t^{TI} is smaller than the experimental value E_t^*. As Table 2 shows and the results therein are not surprising in view of the previous comment: Some data sets do not allow the identification of the stiffness scaler κ for transverse isotropy.

However, if the orthotropic material symmetry assumption holds, as supposed in Refs. [2,16], the interphase stiffness scalar κ in our model may be identified for all data sets. Further experimental investigations are necessary to show, whether the test specimen have privileged axis also perpendicular to the fiber direction. For example the normal direction to the plane of the lamina may be such an axis of material symmetry, since the manufacturing process of the UD-lamina, from which the test specimen is cut out, may cause a compactification of the reinforcing fibers in that direction. This may be the reason for the high values of the experimental results, found for the elastic modulus E_t^* transverse to the fiber in Ref. [2].

For future investigations further test data $()^*$ for the effective material parameters of the composite besides the transverse elasticity modulus E_t^* should be measured in laboratory experiments and used for the identification of the interphase properties. Therefore, it is advisable to measure additionally the axial shear stiffness G_a^* besides the transverse elasticity modulus E_t^* of the composite in the tests, since the axial elastic shear value is also crucially affected by the interphase properties. By means of a second independent stiffness modulus of the composite, furnished by the experiments, the value for the interphase parameter κ may be either improved or verified. Another possibility to improve the results of this identification technique may be the combination of this method based on a homogenisation technique and experimental data for the overall composite properties together with micromechanical experimental investigations like push-out und pull-out tests described by associated models [17,18].

7. Summary

The GMC is applied to identify the elastic properties of the interphase region between the fiber and the matrix in unidirectionally reinforced composite materials. The cells model to approximate an arbitrary geometry of the internal microstructures closely and to determine the overall effective elastic properties of the composite. A unidirectionally fiber-reinforced composite with a thin interphase region is modeled by this advantageous feature. A numerical identification algorithm is developed with the help of a gradient-based optimisation scheme for the inverse determination of the elastic interphase properties, which are related most simply to the matrix stiffness coefficients.

The numerical examples demonstrate the successful application of the identification strategy to various sets of test data. The calculated results for the interphase parameters confirm the good agreement of the analytical homogenisation scheme GMC with the numerical homogenisation by the finite element method, as it could be expected.

Although the interphase parameters are successfully identified from the experimental data for most composites with various chemical treatment of the fiber surface, the numerical results are still not satisfying in all cases. The unsuccessful attempts are those ones, where the calculated values of the interfacial properties are unrealistically high for the fiber-matrix-interphase systems, in case a transverse isotropic material model is assumed for the calculation of the overall composite behaviour. Many more test data are necessary for a more reliable identification of the interphase properties, but the experimental effort is enormously big for the specification of all necessary moduli for the phases and the fiber volume content.

Acknowledgements

The authors gratefully acknowledge the financial support of the Deutsche Forschungsgemeinschaft (DFG) in Bonn through the Graduiertenkolleg ‘Identifikation von Material-und Systemeigenschaften’.

References

[1] Kim J-K, Mai Y-W. Engineered interface in fiber reinforced composites. Oxford: Elsevier; 1998.
[2] Wacker G. Experimentell gestützte Identifikation ausgewählter Eigenschaften glasfaserverstärkter Epoxidharze unter Berücksichtigung der Grenzschicht. PhD Thesis. Department of Mechanical Engineering, University of Kassel, 1996.
[3] Drzal LT, Madhukar M. Fibre-matrix adhesion and its relationship to composite mechanical properties. J Mater Sci 1993;28:569–610.
[4] Larson BK, Drzal LT. Glass fibre sizing/matrix interphase formation in liquid composite moulding: effects on fibre/matrix adhesion and mechanical properties. Composites 1994;25(7):711–21.
[5] Gerlach S. Modellbildung and Parameteridentifikation, Faserverbund-werkstoffe. PhD thesis, Department of Mechanical Engineering, University of Kassel; 2003.
[6] Paley M, Aboudi J. Micromechanical analysis of composites by the generalized cells method. Mech Mater 1992;14:127–39.
[7] Herakovich CT. Mechanics of fibrous composites. 1st ed. New York: Wiley; 1998.
[8] Aboudi J. Micromechanical analysis of composites by the method of cells—update. Appl Mech Rev 1996;49:83–91.
[9] Matzenmiller A, Gerlach S. Micromechanical modeling of viscoelastic composites with complaint fiber–matrix bonding. Comput Mater Sci 2004;29(3):283–300.
[10] Aboudi J. Mechanics of composite materials—a unified micromechanical approach. 1st ed. Amsterdam: Elsevier; 1991.

[11] Spellucci P. DONLP2: SQP/ECQP-method for general continuous nonlinear programming; 2000. [Fortran Routine in] http://www.mathematik.tudarmstadt.de/ags/ag8/Mitglieder/spellucci_de.html.
[12] Sun CT, Vaidya RS. Prediction of composite properties from a representative volume element. Comp Sci Technol 1996;56:171–9.
[13] Altenbach H, Altenbach J, Rikards R. Einführung in die Mechanik Laminat- und Sandwichtragwerke. 1st ed. Stuttgart: Deutscher Verlag für Grundstoffindustrie; 1996.
[14] Aboudi J. Constitutive behavior of multiphase metal matrix composites with interfacial damage by the generalized cells model. In: Voyiadjis GZ, editor. Damage in composite materials. Amsterdam: Elsevier; 1993. p. 3–22.
[15] Arnold SM, Pindera MJ, Wilt TE. Influence of fiber architecture on the inelastic response of metal matrix composites. Int J Plast 1996;12(4): 507–45.
[16] Wacker G, Bledzki AK, Chate A. Effect of interphase on the transverse young's modulus of glass/epoxy composites. Compos Part A 1998;26A: 619–26.
[17] Pompe G, Maeder E. Experimental detection of a transcrystalline interphase in glass–fibre/polypropylene composites. Comp Sci Technol 2000;60:2159–67.
[18] Maeder E, Pisanova E. Characterization and design of interphases in glass fiber reinforced polypropylene. Polym Compos 2000;21(3): 361–8.